

RSC Advances



This is an *Accepted Manuscript*, which has been through the Royal Society of Chemistry peer review process and has been accepted for publication.

Accepted Manuscripts are published online shortly after acceptance, before technical editing, formatting and proof reading. Using this free service, authors can make their results available to the community, in citable form, before we publish the edited article. This *Accepted Manuscript* will be replaced by the edited, formatted and paginated article as soon as this is available.

You can find more information about *Accepted Manuscripts* in the [Information for Authors](#).

Please note that technical editing may introduce minor changes to the text and/or graphics, which may alter content. The journal's standard [Terms & Conditions](#) and the [Ethical guidelines](#) still apply. In no event shall the Royal Society of Chemistry be held responsible for any errors or omissions in this *Accepted Manuscript* or any consequences arising from the use of any information it contains.

Cite this: DOI: 10.1039/c0xx00000x

www.rsc.org/xxxxxx

ARTICLE TYPE

One-step fabrication of robust and optically transparent slippery coatings

V. Anand Ganesh,^a Saman Safari Dinachali,^d Sundaramurthy Jayaraman,^{b,e} Radhakrishnan Sridhar,^{b,c} Hemant Kumar Raut,^a Aleksander Góra,^{b,c} Avinash Baji,^a A. Sreekumaran Nair^{*f} and Seeram Ramakrishna^{*b,c}

Received (in XXX, XXX) Xth XXXXXXXXXX 20XX, Accepted Xth XXXXXXXXXX 20XX

DOI: 10.1039/b000000x

Fabrication of lubricants-infused textured surfaces has opened up a new route towards omniphobicity. However, achieving a homogeneous thin film of lubricating material on a flat/smooth surface still remains a challenge. This work shows the successful fabrication of thin, transparent, and homogeneous coating of perfluoropolyether (PFPE, a lubricating material) on a smooth glass surface by electro spraying technique. The sol-gel solution for electro spraying is prepared by adding a small amount of (tridecafluoro-1,1,2,2-tetrahydrooctyl)-1-trichlorosilane (FTS) with PFPE and subsequently electro sprayed on the glass substrate. After curing the coated samples at 80 °C, a transparent, homogeneous, and slippery coating with low surface energy (12.5 mN/m) is obtained. It is observed that the presence of FTS with PFPE, assisted significantly in stacking of PFPE on the substrate resulting in the formation of smooth, uniform blended (PFPE + FTS) films. The surface nature of the blended films is characterized by spectroscopy and microscopy. The blended surface exhibits omniphobic property with surface contact angles and slipping angles achieved using water and acetone are found to be (116°, 40.8°) and (6°, 10°), respectively. Furthermore, the coating shows good optical (transmittance: 91%) and mechanical properties with strong adherence to glass surface, thus revealing the potential for applications in windows and solar modules.

1. Introduction

Self-cleaning, anti-icing, anti-microbial, corrosion resistant, and oil-repellent surfaces have engrossed the attention of researchers around the world and extensive research works are being carried out in this area to maximize the operational efficiency of automobiles, aircrafts, marine vessels, wind turbines, architectural glasses/materials, photovoltaic glasses, and filtration/purification processes.¹⁻¹⁰ Inspired by naturally occurring self-cleaning surfaces such as lotus/rice leaves, bird's feathers, butterfly wings, water strider's legs, etc. numerous self-cleaning superhydrophobic surfaces have been developed in recent times by the combination of low surface energy materials with different surface textures.¹¹⁻¹⁵ However, the advancement in the field of designing oleophobic/superoleophobic surfaces is relatively slow. This is because the surface tension of non-polar liquids is very low; hence engineering surfaces that can de-wet these liquids involves complicated micro/nano structures designs, overhangs, and re-entrant surface curvatures.¹⁶⁻²² In addition to the substrate-dependent design complications, lotus-leaf inspired surfaces also face the issue of optical transparency. The surface roughness that induces hydrophobicity/oleophobicity generally lessens the light transmitting property of the surface. To overcome this issue, transparent superhydrophobic surfaces are prepared by introducing nanostructures with dimensions less than

100 nm.²³⁻²⁵ Nonetheless, these structures do not allow the formation of stable air cushion beneath the liquid droplets resulting in the reduction of robustness of the surface. To address these needs and to overcome the limitations of lotus-leaf inspired topographically modified surfaces, a new type of slippery surfaces with low contact angle hysteresis have been developed recently.²⁶⁻³⁰ In contrast to the superhydrophobic surfaces, slippery surfaces do not rely on the air trapping mechanism for liquid repellency. Instead, these surfaces use a thin layer of lubricating material that offers a smooth, transparent, and homogeneous interface which provides an exceptional slippery surface to a broad range of liquids.²⁷⁻³⁰

Herein, we report a simple and scalable approach to fabricate a robust, transparent, and slippery surface for both polar and non-polar liquids. We have employed electro spraying technique to produce a thin layer of PFPE on a smooth glass surface to achieve omniphobicity (ability to repel water and organic solvents). In this method, the liquid dispensing nozzle (needle) is maintained at a very high electrical potential and hence liquid at the outlet of the needle is subjected to an electrical shear stress. As a result, the droplet sprayed onto the substrate can be very small and the size of the droplet can be controlled by adjusting the flow-rate and the voltage applied to the needle.^{31,32} This technique can deposit nanoparticles on large scale with a simple set-up containing the sol-gel solution, a collector and high voltage power supply. The electro spraying technique has the following

advantages over the conventional mechanical atomizer (such as the spray coating): 1) the droplet size is smaller than that available from conventional spray processes, and can be in the nanometer range, 2) the standard deviation of the size distribution of droplets is usually small that allows production of particles of nearly uniform size, 3) the charged droplets are self-dispersing in space (due to their mutual repulsion) and thus droplet coagulation is absent, and 4) motion of the charged droplets can be controlled by electric field allowing focusing the aerosol on the substrate.^{31,32}

To achieve a homogeneous coating of pure PFPE on a flat surface is difficult, due to the poor adhesion of PFPE with the surface (glass/silicon).³³ In present work, we have addressed this issue by adding a small amount of FTS ((tridecafluoro-1,1,2,2-tetrahydrooctyl)-1-trichlorosilane) with PFPE. FTS facilitates the stacking of PFPE with the substrate, resulting in the formation of a homogeneous, transparent, thin blended (PFPE + FTS) layer over the substrate. The transmittance of the coating is around 91% and the surface contact angles achieved using conc. NaOH (sodium hydroxide, $\gamma = 85$ mN/m), water ($\gamma = 72.1$ mN/m), conc. H₂SO₄ (sulphuric acid, $\gamma = 55.1$ mN/m), and acetone ($\gamma = 23.1$ mN/m) are measured to be 119°, 116°, 99.5° and 40.8°, respectively.

2. Experimental section

2.1. Materials

Perfluoropolyether (PFPE) (Fomblin, Sigma-Aldrich, Mw = 2500 g/mol), (tridecafluoro-1,1,2,2-tetrahydrooctyl)-1-trichlorosilane (FTS, Alfa Aesar, 97%), iso-propanol, ethanol, methanol, acetone, chloroform, acetic-acid, toluene, *N,N*-dimethyl formamide (DMF), ethylene glycol, glycerol, di-iodomethane, hexadecane, dodecane, conc. sulphuric acid (95-97%), conc. sodium hydroxide (1 M solution), hydrogen peroxide (31% H₂O₂ with 69% water) (all from Aldrich), and de-ionized water were used without any further purification.

2.2. Solution and substrate preparation

The sol-gel solution for electrospaying was prepared as follows: an optimized proportion of about 25 μ L (0.0675 mM) of FTS was added to 2 mL (1.52 mM) of PFPE (we have measured the surface contact angle and optical transmittance of the thin films fabricated using higher molar ratios of FTS with PFPE). As the values were very similar, we have concluded that 25 μ L of FTS in 2 mL of PFPE is the optimum proportion for thin film formation (please refer **Table ST1**.)

Slide glass plates (24 mm \times 24 mm \times 1.2 mm) were thoroughly cleaned by ultra-sonication in de-ionized water and acetone, respectively, for about 15 min each. To ensure that the glass slides were free from surface contaminants, they were cleaned with Piranha solution (3:7 by volume of 30% H₂O₂ and H₂SO₄) for 2 h followed by rinsing in de-ionized water. The cleaned glass plates were dried in an oven at 80 °C for 15 min.

2.3. Electrospaying

The sol-gel solution was loaded into the electrospinning/spraying machine (NANON, MECC- Japan). The washed and dried microscopic glass slides were then mounted on a flat collector wrapped with aluminium (Al) foil. The applied voltage was set to

30 kV and the distance between the needle (27G 1/2) tip and the static collector was set to 10 cm. The humidity level in the electrospaying chamber was maintained between 50 and 60%. The FTS-PFPE solution is electrospayed on the glass substrates for 20 min with the flow-rate of about 1 mL h⁻¹ to deposit a uniform layer of FTS-PFPE on the glass substrate. The coated surfaces were subsequently annealed at 80 °C for 3 h and then subjected to characterization.

3. Characterization

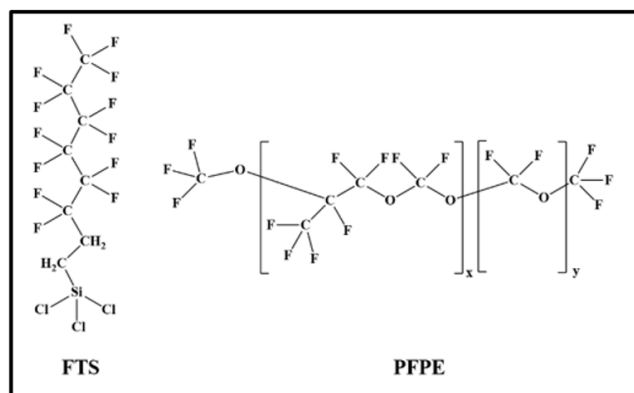
The samples for scanning electron microscopy (SEM) were platinum sputtered and the images were captured using a field emission SEM instrument (JEOL, JSM-6700F) operated at 5 kV. The thickness of the film was measured by a surface profiler (Alpha-Step IQ Surface Profiler). The contact angle measurements (static, advancing, receding and slipping angles) were carried out using a contact angle measurement setup (VCA optima contact angle equipment from AST Products) in static/dynamic sessile drop mode at room temperature. The surface contact angle values reported were the averages of at least ten measurements made on different areas of the coated sample. The transmittance was measured using a Shimadzu SolidSpec 3700 UV-vis-NIR Spectrometer. Atomic Force Microscopic (AFM) images of the coated samples were taken using an Atomic Microscope Nanowizard 3 machine (JPK, Germany). X-ray photoelectron spectroscopy (XPS) was done using AXIS-HSi spectrometer (Kratos Analytical). Al K α X-ray radiation ($h\nu = 1486.6$ eV) was employed with an incident angle of 30° and collected at a take-off angle of 50° with respect to the surface normal. The analysis area and analysis depth were nearly 400 nm and 10 nm, respectively. Survey spectrum and high-resolution spectra of elements were acquired for elemental composition analysis and identification of oxidation state of the elements. Low energy electron flooding was adopted for charge compensation and carbon correction was made using the standard software from the manufacturer.

4. Results and discussion

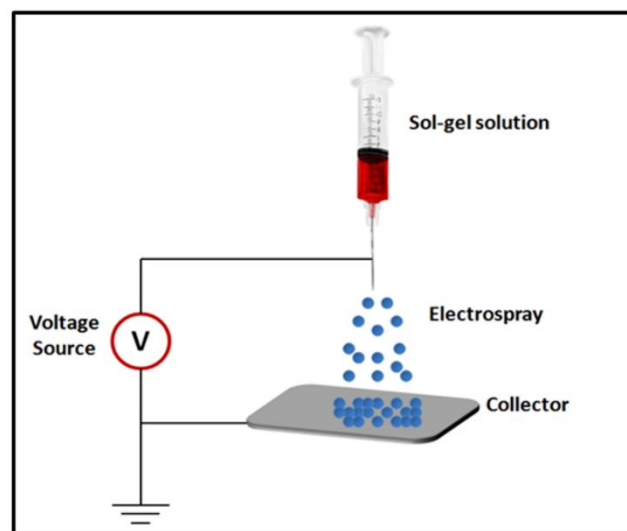
PFPE is nontoxic, biologically inert, fire resistant and highly transparent lubricating liquid with a very low surface tension and volatility. It is immiscible with both aqueous and hydrocarbon phases (see **Scheme 1** for the structure of PFPE employed). Hence it can form a stable interface with several polar and non-polar liquids. This material is, therefore, chosen for fabricating transparent omniphobic surface by electrospaying process. However, as explained by Ma *et al.*, it is difficult to achieve a stable homogeneous thin film of PFPE on a flat surface.³³

To overcome this issue, we have added a small amount of FTS (see **Scheme 1** for the structure) with PFPE. A homogenous solution was obtained after addition and mixing of FTS. Both FTS and PFPE possess -CF₂- in the backbone chain which results in Van der-Waal's force of attraction between them. This force of attraction assists FTS molecules to mix uniformly with PFPE and coil along the backbone chains. The solution was then electrospayed (see **Scheme 2**) on a glass substrate followed by curing at 80 °C for 3 h resulting in the formation of a smooth (surface roughness: < 5 nm) homogeneous, transparent and thin

(thickness: 180 ± 20 nm approx.) blended (PFPE + FTS) surface over the glass substrate.



Scheme 1. Chemical structure of FTS and PFPE.

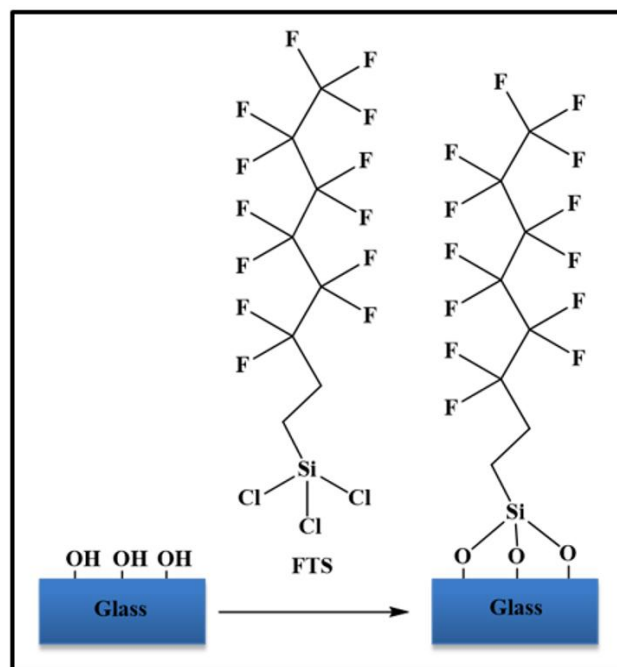


Scheme 2. Schematic representation of electro spraying set-up employed.

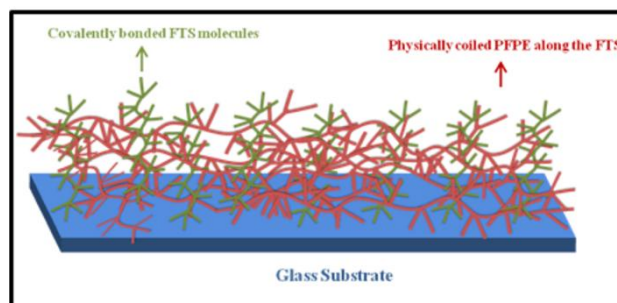
The interaction mechanism between PFPE and FTS on the substrate is explained as follows: The FTS molecules that are present uniformly along with the PFPE possess highly reactive trichlorosilane end groups. Upon electro spraying the mixed solution on glass, the trichlorosilane end groups are hydrolysed (**Scheme 3**) and gets covalently bonded with the substrate by formation of Si-O-Si bond.³⁴ Consequently, the PFPE coiled along with the FTS due to Van der-Waals's force of attraction also get stacked onto the substrate (**Scheme 4**). During thermal annealing, the air pockets and other residues will be removed; resulting in the formation of a compact and dense layer of FTS + PFPE blended film. The excess and unbounded materials are removed from the substrate by ultra-sonication.

A comparison of the FTIR spectra of PFPE, FTS and their mixture reveals the presence of PFPE with FTS on the substrate (**Figure S1**). The IR spectrum of the mixture showed shifts and broadening of peaks at 1265 cm^{-1} , 1198 cm^{-1} and 1149 cm^{-1} , respectively, which are due to the presence of PFPE with the highly reactive FTS. While the peaks at 1265 cm^{-1} and 1198 cm^{-1} are corresponding to the C-F vibrations, the peak at 1149 cm^{-1}

could be due to Si-O-Si bond formation between the PFPE + FTS mixture and the substrate.



Scheme 3. Interaction of highly reactive trichlorosilane end groups with the substrate.



Scheme 4. Schematic illustration of interaction mechanism between FTS, PFPE and glass substrate.

In order to have a better understanding about the thin film formation, XPS characterization has been carried out. **Figure 1a** shows the high resolution XPS spectra of C1s. The C peak at 286.1 eV is indicative of the C in the functional group ($-\text{C}-\text{CF}_2-$) present along the backbone chain of FTS and PFPE.³⁵ The C in the functional groups ($-\text{O}-\text{CF}_2-$) and ($-\text{O}-\text{CF}_2-\text{O}-$) present in the PFPE are confirmed by the peaks at 291.1 eV and 293.4 eV , respectively (**Figure 1a**).³⁶ These highly prominent peaks confirm the presence of PFPE with FTS even after sonication and inducing the omniphobic property.

Figure 1b shows the XPS scan of oxygen (O1s). The O1s core level peak is located at 532.2 eV and the less intense shake-up peak at 535.6 eV is associated to oxygen atoms in the PFPE molecule.³⁵ The XPS scan of F1s confirms the presence of fluorine (peak at 688.4 eV) (**Figure 1c**) and wide scan spectrum of the blended film of PFPE and FTS further confirmed the elemental composition (**Figure 1d**).

Cite this: DOI: 10.1039/c0xx00000x

www.rsc.org/xxxxxxx

ARTICLE TYPE

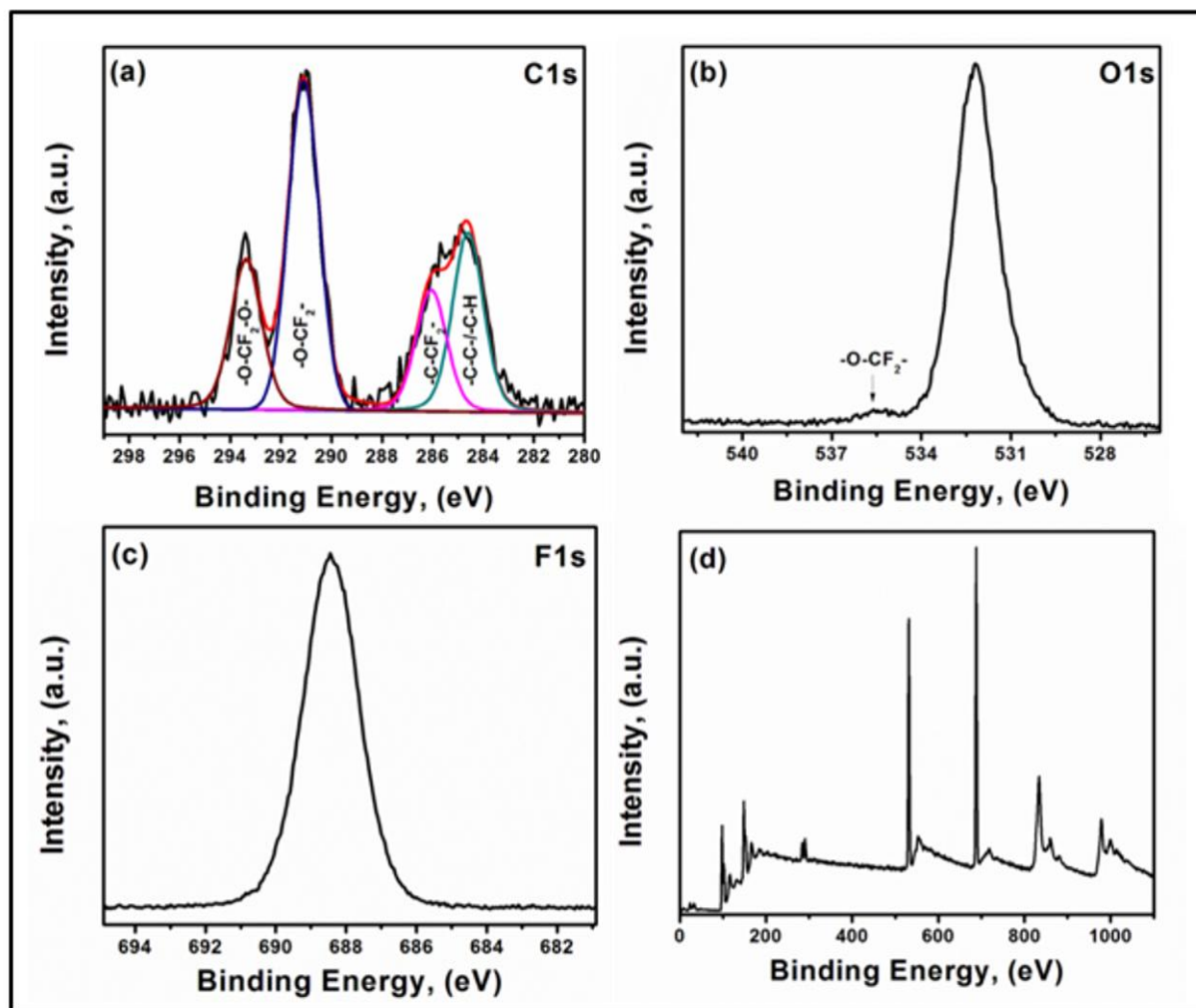


Figure 1. XPS spectra of electrospayed FTS and PFPE blended films after sonication: (a) C1s, (b) O1s, (c) F1s and (d) wide spectrum.

Figure 2 (a), (b), (c) and (S2) show the optical microscope, SEM and AFM images, respectively, of the coated sample (coated with FTS and PFPE mixture) exhibiting a homogenous and uniform film over the glass substrate. Figure 3 shows the optical microscope images of the electrospayed samples with and without the addition of FTS in PFPE. It is observed that the pure PFPE coating gets de-wetted from the glass surface (Figure 3). On the other hand, the presence of FTS has induced the stacking of PFPE layers, resulting in the formation of a continuous and uniform thin film (Figure 3). As is evident from the proposed interaction mechanism (Scheme 3, 4), in a blended surface, the low surface energy group tends to move to the surface which facilitates a decrement in the overall free energy of the system.^{37,38} These blended thin films exhibited omniphobic property.

The contact angle and sliding angle (SA) made by water

droplet (2 μ L) on the coated sample were measured to be $116^\circ \pm 2.5$ and $6^\circ \pm 0.6$, respectively. Besides water repellency, the coated surface also exhibited excellent repellency for non-polar liquids and even for some solvents like acetone, chloroform, toluene and ethanol. The surface contact angle (SCA), sliding angle and the advancing (θ_a)/receding angles (θ_r) were measured for several liquids with different surface tension values by using a “tilting base contact angle measurement set-up” and contact angle hysteresis (CAH) was calculated by taking the difference of advancing and receding angles (Table 1; Figure 4). The CAH achieved for water, acetone, conc. H_2SO_4 and conc. NaOH was measured to be 5, 8, 7 and 5° , respectively. The drops (2 μ L) of acetone and ethanol can slip at very low tilting angles (10°).

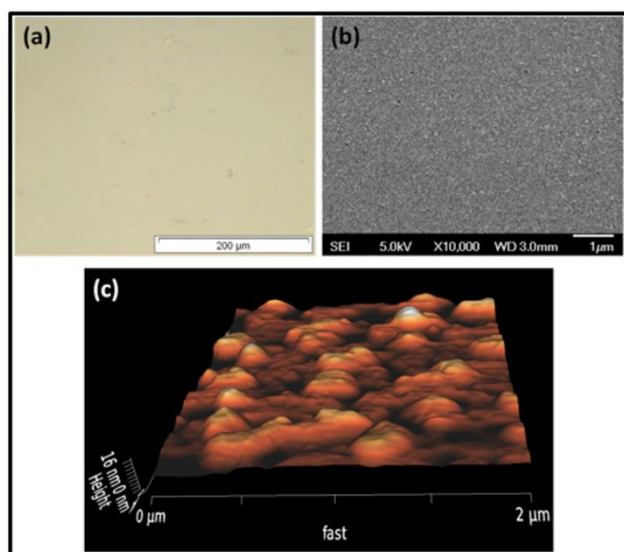


Figure 2. Images of electrospayed PFPE + FTS blended surface. (a) Optical microscopic; (b) SEM; (c) AFM images.

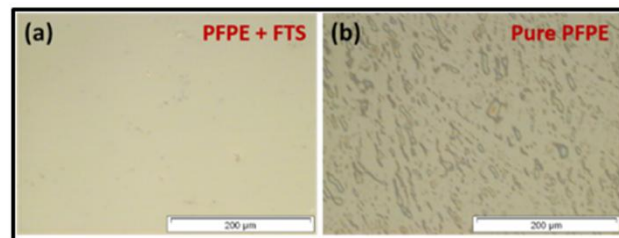


Figure 3. Optical microscopic images of (a) electrospayed PFPE + FTS blended surface; (b) electrospayed pure PFPE surface.

However, the slipping rate strongly depends on the value of tilting angles. We believe that the exceptional de-wetting behaviour of the coated surface is primarily due to the immiscible property of PFPE with various liquids and also the high chain mobility of PFPE.^{29,33}

The surface energy exhibited by the omniphobic surface was calculated using Owens-Wendt and Fowkes equation.^{39,40}

$$\frac{[\sigma_L (\cos \theta + 1)]}{2} = \overline{\sigma_{PS}} \overline{\sigma_{PL}} + \overline{\sigma_{DS}} \overline{\sigma_{DL}} \quad \text{----- (1)}$$

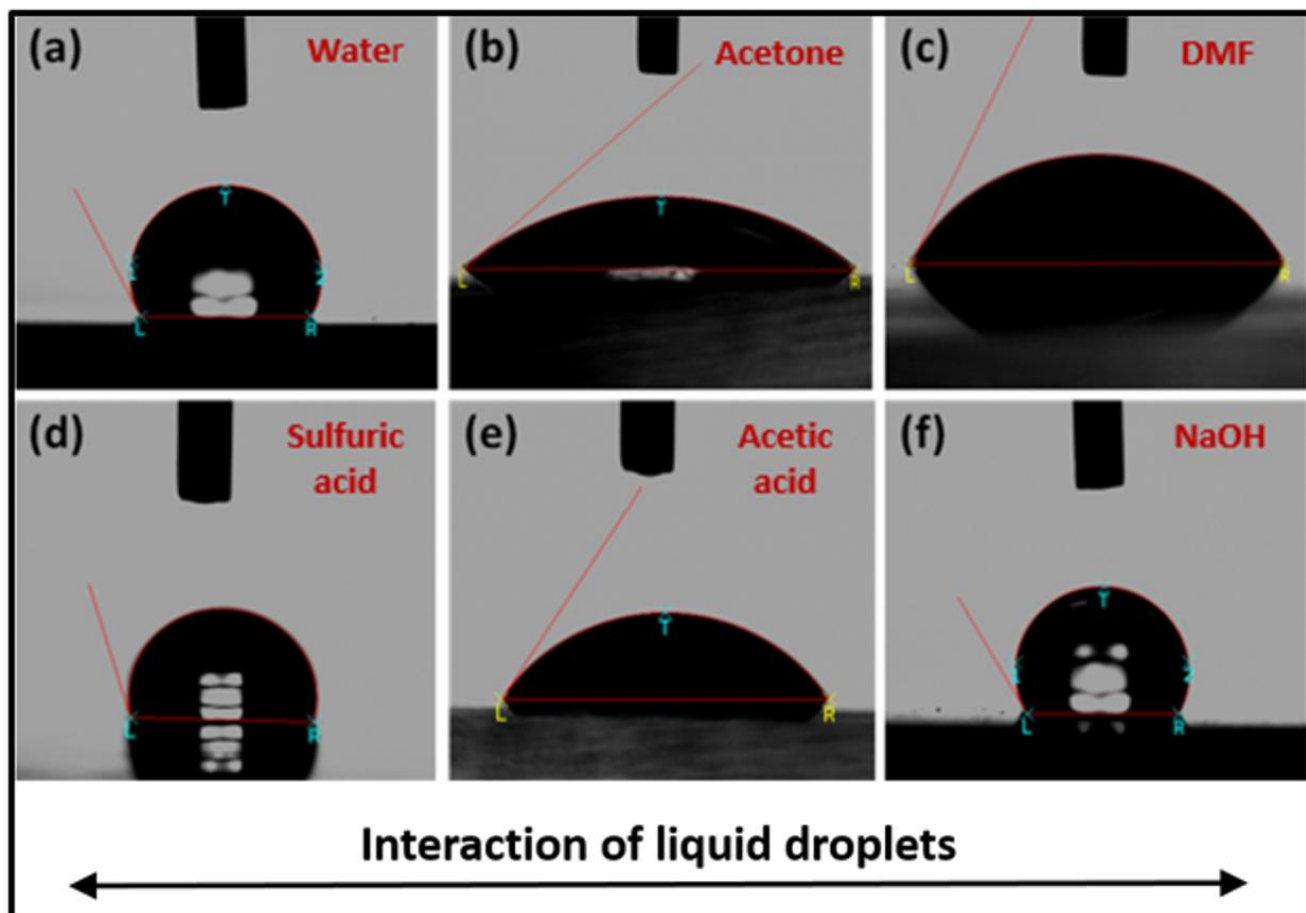


Figure 4. Interaction of liquid droplets with different surface tension. (a) Water (WCA: 116°); (b) Acetone (SCA: 40.8°); (c) *N,N*-dimethyl formamide (SCA: 68.6°); (d) conc. sulphuric acid (SCA: 99.5°); (e) conc. acetic acid (SCA: 55.8°); (f) conc. sodium hydroxide (SCA: 119°).

Cite this: DOI: 10.1039/c0xx00000x

www.rsc.org/xxxxxxx

ARTICLE TYPE

Table 1. Surface contact angle and sliding angle measurements of liquids with different surface tension on an omniphobic-coated glass substrate.

Liquid	Surface Tension (mN/m)	Surface contact angle (SCA) (degrees)*	Sliding angle (Slipping angle) (SA) (degrees)*	Contact Angle Hysteresis (CAH) (degrees)
Isopropanol	20.9	36.5	10	10
Ethanol	21.8	37.3	10	9
Methanol	22.5	39.1	10	9
Acetone	23.1	40.8	10	8
Dodecane	25.3	41.9	9	8
Chloroform	27.1	43.2	9	8
Acetic acid	27.3	55.8	10	8
Hexadecane	27.4	62.4	10	8
Toluene	28.5	61.7	9	8
<i>N,N</i> -dimethyl formamide	37.1	68.6	8	7
Ethylene glycol	48.2	77.2	8	7
Di-iodomethane	50.8	89.5	8	7
Conc. sulfuric acid	55.1	99.5	8	7
Glycerol	64	107.5	7	5
Water	72.8	116	6	5
Conc. hydrogen peroxide	79.7	117.5	5	5
Conc. sodium hydroxide	85	119	5	5

⁵ Volume of droplets used for measurements: 2 μ L.

* SCA/SA values reported are the averages of at least ten measurements made on different areas of the coated sample.

In the above equation, σ_{PS} and σ_{DS} represent the polar and dispersive components of the coated samples. The sum of these two components gives the total surface energy (σ_s) of the coated sample. σ_{PL} and σ_{DL} represent the polar and dispersive components of the probe liquids (water and di-iodomethane,

respectively, in the present case). σ_L represents the total surface tension of the probe liquid used for the measurements. ' θ ' represents the measured static contact angle made by the probe liquids on coated glass samples. Measured static contact angle (θ) and standard surface tension values of polar (σ_{PL}) and dispersive

components (σ_{DL}) of water and di-iodomethane were substituted in equation (1) which resulted in the formation of two equations with two unknowns (σ_{PS} and σ_{DS}). By solving the two equations, values of polar (σ_{PS}) and dispersive components (σ_{DS}) were obtained and sum of the obtained values gave the surface energy of the omniphobic surface (σ_S). The static contact angle values made by water and di-iodomethane droplets on the omniphobic surface were 116° and 89.5° , respectively. Hence the surface energy of the omniphobic surface was calculated to be (σ_S) 12.5 ± 0.5 mN/m.

A comparison of the UV-Vis spectra (in transmittance mode) of plain glass and omniphobic-coated glass sample is shown in **Figure 5**. Results indicated that the transmittance values of plain glass and omniphobic glass were very similar (around 91%) for the entire wavelength range (300-1200 nm). This further implies that the coating did not affect the optical properties of the glass (mainly the light transmittance), which makes this coating suitable for applications in window and solar modules. We have also coated the sol-gel solution on silicon substrate and studied the omniphobic property (**Table ST2**, inset in **Figure 5**). It was observed that the coating remained stable and exhibited omniphobic property irrespective of the type and nature of the substrate over which it was coated. Hence, we believe that the coating is suitable for industrial and commercial applications as well; however, this needs to be explored in future.

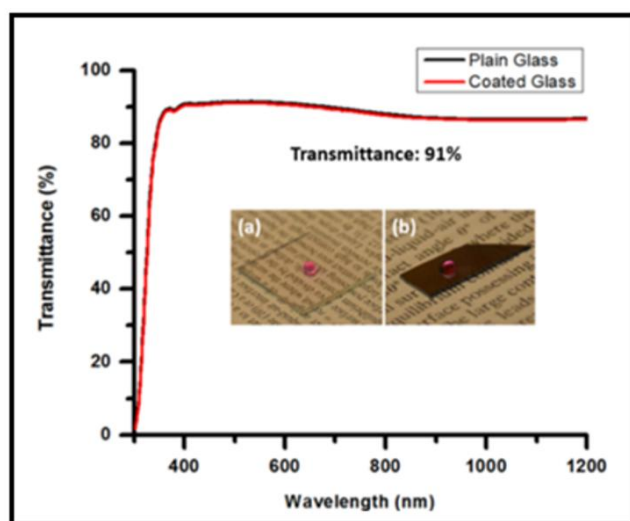


Figure 5. Comparison of the transmittance of the plain and omniphobic-coated glass samples. Inset shows the photograph of glycerol droplets (pink - dyed with rhodamine B) on the omniphobic surfaces fabricated on different substrates; (a) coated glass (b) coated silicon.

A 90° peel-off test was conducted on the coated sample (**Figure S3**) using an adhesion tape (3M scotch tape). The tape was peeled-off from the coated surface (test distance: 40 mm) by applying a fixed force of 5 ± 0.1 N. After the peel-off test, it was observed that the coating remained stable. The samples before and after peel-off test were imaged under optical microscope, SEM and AFM, respectively. The images confirmed that there were no changes even in micrometer scale regimes (**Figure 6**). In order to further confirm the presence of coating after peel-off test, contact angle and sliding angle measurements were carried out in the area where the test was conducted. It was observed that the

coating remained stable and also exhibited the omniphobic properties (**Table ST3**).

Furthermore, spin coating experiment was also conducted to study the stability of the coating on the glass substrate under mechanical forces. The optimised sol-gel solution containing FTS and PFPE is spin-coated (speed - 3000 rpm; duration - 30 s) on the glass substrate and subsequently annealed at 80°C for 3 h (excess materials were removed from the substrate by ultrasonication). After annealing, the contact angle and sliding angle measurements were carried out using water and acetone droplets ($2\ \mu\text{L}$) on the coated substrate. It was observed that the coating remained stable exhibiting omniphobic property with contact angles measured for water and acetone droplets were (114° , 39°), respectively. The sliding angles made by water and acetone droplets were measured to be (7° , 10°), respectively.

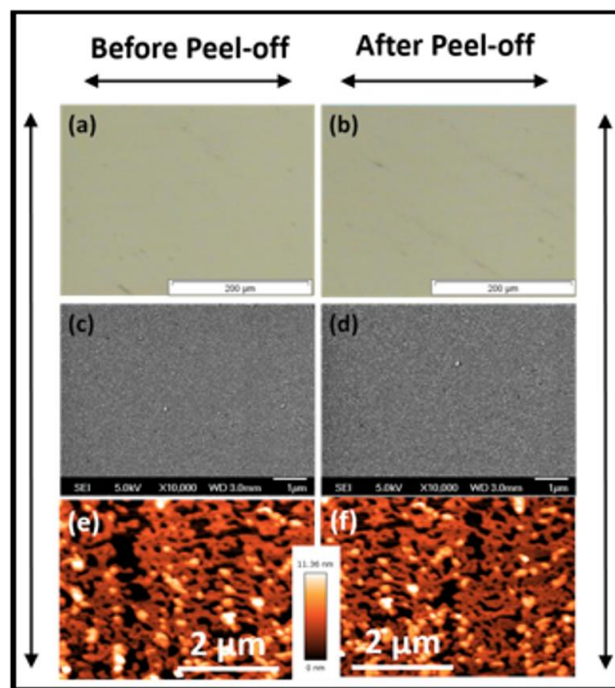


Figure 6. Optical microscopic images (a) before peel-off test; (b) after peel-off test; SEM images (c) before peel-off test; (d) after peel-off test; AFM images (e) before peel-off test; (f) after peel-off test; The SEM, AFM and optical microscopic images further confirm that the coating remained stable after peel-off test.

The coated samples were kept in an environment which was maintained at standard ambient temperature and pressure condition (temperature: $25 \pm 2^\circ\text{C}$; pressure: 0.986 atm; humidity: 40-60%).⁴¹ Surface contact angle measurements for water and acetone were carried out on bi-weekly basis (**Table ST4**). The results indicated that the coating is environmentally stable and retained the omniphobic property.

5. Conclusions

In summary, we have fabricated a thin, transparent and homogeneous coating of PFPE on a glass surface by electrospaying technique. It is difficult to produce a homogeneous coating of PFPE alone on a flat surface due to the poor adhesion of PFPE with the surface (glass/silicon). This issue

was addressed by adding a small amount of FTS with PFPE. The FTS facilitated stacking of PFPE layers, resulting in the formation of homogeneous, transparent, and slippery surface. The PFPE + FTS blended surface was characterized by spectroscopy and microscopy. The coated surfaces (PFPE and FTS blended surface) exhibited omniphobic property with surface contact angle values with conc. NaOH, water, conc. H₂SO₄, and acetone being 119°, 116°, 99.5° and 40.8°, respectively. The coatings were transparent and exhibited strong adhesion with the glass substrate, thus revealing the potential for applications in windows and solar modules.

Acknowledgements

The authors, VAG and AB would like to acknowledge the financial support from Ministry of Education (MOE - Tier 2), Singapore [Grant T2-MOE-1302]. The authors would like to thank Dr. Murugan, Dr. Molamma, Dr. Naveen Kumar and Ms. Anjusree for helpful discussions.

Notes

^a Division of Engineering Product Development, Singapore University of Technology and Design (SUTD), Singapore - 138682.

^b Department of Mechanical Engineering, National University of Singapore, Singapore - 117575.

^c Centre for Nanofibers & Nanotechnology, Nanoscience and Nanotechnology Initiative, National University of Singapore, Singapore - 117576. **Email:** seeram@nus.edu.sg

^d Institute of Materials Research and Engineering (IMRE), Agency for Science, Technology and Research, 3 Research Link, Singapore - 117602.

^e Environmental & Water Technology, Centre of Innovation, Ngee Ann Polytechnic, Singapore - 599489.

^f Amrita Centre for Nanosciences, Amrita Institute of Medical Sciences, Amrita Vishwa Vidyapeetham, AIMS Ponekkara P.O., Kochi - 682041, Kerala, India. **Email:** sreekumarannair@aims.amrita.edu

[†]Electronic Supplementary Information (ESI) available: [FT-IR Spectra of PFPE, FTS and FTS + PFPE surfaces; AFM images of plain glass and PFPE + FTS blended surface; Peel-off test results; Contact angle, sliding angle and transmittance values as a function of amount of FTS added with PFPE; Spin-coating experiment]. See DOI: 10.1039/b000000x/

References

1. V. A. Ganesh, H. K. Raut, A. S. Nair and S. Ramakrishna, *J. Mater. Chem.* 2011, **21**, 16304-16322.
2. W. Choi, A. Tuteja, S. Chhatre, J. M. Mabry, R. E. Cohen and G. H. McKinley, *Adv. Mater.* 2009, **21**, 2190-2195.
3. P. Kim, T. S. Wong, J. Alvarenga, M. J. Kreder, W. E. Adorno-Martinez and J. Aizenberg, *ACS Nano* 2012, **6**, 6569-6577.
4. X. Yao, Y. Song and L. Jiang, *Adv. Mater.* 2011, **23**, 719-734.
5. L. Mishchenko, B. Hatton, V. Bahadur, J. A. Taylor, T. Krupenkin and J. Aizenberg, *ACS Nano* 2010, **4**, 7699-7707.
6. A. J. Meuler, G. H. McKinley and R. E. Cohen, *ACS Nano* 2010, **4**, 7048-7052.
7. V. A. Ganesh, A. S. Nair, H. K. Raut, T. M. Walsh and S. Ramakrishna, *RSC Adv.* 2012, **2**, 2067-2072.
8. V. A. Ganesh, S. S. Dinachali, H. K. Raut, T. M. Walsh, A. S. Nair and S. Ramakrishna, *RSC Adv.* 2013, **3**, 3819-3824.
9. V. A. Ganesh, S. S. Dinachali, A. S. Nair and S. Ramakrishna, *ACS Appl. Mater. Interfaces* 2013, **5**, 1527-1532.
10. S. Pan, A. K. Kota, J. M. Mabry and A. Tuteja, *J. Am. Chem. Soc.* 2012, **135**, 578-581.
11. P. Roach, N. J. Shirtcliffe and M. I. Newton, *Soft Matter* 2008, **4**, 224-240.
12. D. Byun, J. Hong, J. H. Ko, Y. J. Lee, H. C. Park, B. K. Byun and J. R. Lucks, *J. Bionic Eng.* 2009, **6**, 63-70.
13. Z. Z. Luo, Z. Z. Zhang, L. T. Hu, W. M. Liu, Z. G. Guo, H. J. Zhang and W. J. Wang, *Adv. Mater.* 2008, **20**, 970-974.
14. V. A. Ganesh, A. S. Nair, H. K. Raut, T. T. Yuan Tan, C. He, S. Ramakrishna and J. Xu, *J. Mater. Chem.* 2012, **22**, 18479-18485.
15. A. B. D. Cassie and S. Baxter, *Trans. Faraday Soc.* 1944, **40**, 546-551.
16. Tuteja, W. Choi, M. L. Ma, J. M. Mabry, S. A. Mazzella, G. C. Rutledge, G. H. McKinley, and R. E. Cohen, *Science* 2007, **318**, 1618-1622.
17. Tuteja, W. Choi, J. M. Mabry, G. H. McKinley, and R. E. Cohen, *Proc. Natl. Acad. Sci., U.S.A.* 2008, **105**, 18200-18205.
18. W. Wu, X. Wang, D. Wang, M. Chen, F. Zhou, W. Liu, and Q. Xue, *Chem. Commun.* 2009, 1043-1045.
19. H. Butt, C. Semprebon, P. Papadopoulos, D. Vollmer, M. Brinkmann and M. Ciccotti, *Soft Matter* 2013, **9**, 418-428.
20. A. Steele, I. Bayer, and E. Loth, *Nano Lett.* 2008, **9**, 501-505.
21. Z. Xue, M. Liu, and L. Jiang, *J. Polym. Sci., Part B: Polym. Phys.* 2012, **50**, 1209-1224.
22. J. Zhang, and S. Seeger, *Angew. Chem., Int. Ed.* 2011, **50**, 6652-6656.
23. R. G. Karunakaran, C.-H. Lu, Z. Zhang, and S. Yang, *Langmuir* 2011, **27**, 4594-4602.
24. H. Yabu, and M. Shimomura, *Chem. Mater.* 2005, **17**, 5231-5234.
25. P. A. Levkin, F. Svec, and J. M. J. Fréchet, *Adv. Funct. Mater.* 2009, **19**, 1993-1998.
26. (a) T. S. Wong, S. H. Kang, S. K. Y. Tang, E. J. Smythe, B. D. Hatton, A. Grinthal, and J. Aizenberg, *Nature* 2011, **477**, 443-447. (b) A. K. Epstein, T. S. Wong, R. A. Belisle, E. M. Boggs, and J. Aizenberg, *Proc. Natl. Acad. Sci. U. S. A.*, 2012, **109** (33), 13182-13187.
27. (a) F. Cheng, C. Urata, M. Yagihashi, and A. Hozumi, *Angew. Chem., Int. Ed.* 2012, **51**, 2956-2959. (b) X. Yao, Y. Hu, A. Grinthal, T. S. Wong, L. Mahadevan and J. Aizenberg, *Nat. Mater.*, 2013, **12**, 529-534.
28. J. W. Krumpfer, and T. J. McCarthy, *Faraday Discuss.* 2010, **146**, 103-111.
29. P. Kim, M. J. Kreder, J. Alvarenga, and J. Aizenberg, *Nano Lett.* 2013, **13**, 1793-1799.
30. N. Vogel, R. A. Belisle, B. Hatton, T. Wong and J. Aizenberg, *Nat Commun.* 2013, **4**, 2176.
31. N. Bock, M. A. Woodruff, D. W. Hutmacher, and T. R. Dargaville, *Polymers* 2011, **3**, 131-149.
32. A. Jaworek and A. T. Sobczyk, *J. Electrostat.* 2008, **66**, 197-219.
33. W. Ma, Y. Higaki, H. Otsuka, and A. Takahara, *Chem. Commun.* 2013, **49**, 597-599.
34. H. Xiang and K. Komvopoulos, *J. Appl. Phys.* 2013, **113**, 224505.
35. P. Fabbri, M. Messori, M. Montecchi, S. Nannarone, L. Pasquali, F. Pilati, C. Tonelli and M. Toselli, *Polymer* 2006, **47**, 1055-1062.
36. L. Li, Y. Wang, C. Gallaschun, T. Risch and J. Sun, *J. Mater. Chem.* 2012, **22**, 16719-16722.
37. P. A. V. O'Rourke-Muisene, J. T. Koberstein and S. Kumar, *Macromolecules* 2003, **36**, 771-781.
38. E. Suk, G. Chowdhury, T. Matsuura, R. M. Narbaitz, P. Santerre, G. Pleizier and Y. Deslandes, *Macromolecules* 2002, **35**, 3017-3021.

-
39. D. K. Owens, and R. C. Wendt, *J. Appl. Polym. Sci.* 1969, **13**, 1741-1747.
 40. M. Fowkes, M. B. Kaczinski, and D. W. Dwight, *Langmuir* 1991, **7**, 2464-2470.
 - 5 41. J. Phys. Chem. Ref. Data 1982, 11 (Supplement 2).